ORIGINAL ARTICLE

Esophageal mycobiome landscape and interkingdom interactions in esophageal squamous cell carcinoma

Wen-Qing Rao[1],[†], Zheng Lin[1],[†], Jian Jiang[1],[2], Jian-Wen Wang[3], Zhi-Feng Lin[1], Rong Fu[1], Wei-Lin Chen[4], Yuan-Mei Chen[5], Xian-E. Peng [ID] [1] and Zhi-Jian Hu[1],[6],[*]

[1]Department of Epidemiology and Health Statistics, Fujian Medical University Fujian Provincial Key Laboratory of Environment Factors and Cancer, School of Public Health, Fujian Medical University, Fuzhou, Fujian, P. R. China, [2]Department of Medical Services, Fujian Provincial Hospital, Fuzhou, Fujian, P. R. China, [3]Department of Digestive Endoscopy, Anxi County Hospital, Anxi, Fujian, P. R. China, [4]Department of Radiation Oncology, Zhangzhou Affiliated Hospital of Fujian Medical University, Zhangzhou, Fujian, P. R. China, [5]Department of Thoracic Surgery, Fujian Provincial Cancer Hospital Affiliation to Fujian Medical University, Fuzhou, Fujian, P. R. China; [6]Key Laboratory of Ministry of Education for Gastrointestinal Cancer, Fujian Medical University, Fuzhou, Fujian, P. R. China

*Corresponding author. Department of Epidemiology and Health Statistics, Fujian Provincial Key Laboratory of Environment Factors and Cancer, School of Public Health, Key Laboratory of Ministry of Education for Gastrointestinal Cancer, Fujian Medical University, Fuzhou, Fujian 350122, China. Tel: +86-591-83383362; Fax: +86-591-22862510; Email: huzhijian@fjmu.edu.cn
[†]These authors contributed equally to this work.

Abstract

Background   The study purpose was to characterize the mycobiome and its associations with the expression of pathogenic genes in esophageal squamous cell carcinoma (ESCC).

Methods   Patients with primary ESCC were recruited from two central hospitals. We performed internal transcribed spacer 1 (ITS1) ribosomal DNA sequencing analysis. We compared differential fungi and explored the ecology of fungi and the interaction of bacteria and fungi.

Results   The mycobiota diversity was significantly different between tumors and tumor-adjacent samples. We further analysed the differences between the two groups, at the species level, confirming that *Rhodotorula toruloides*, *Malassezia dermatis*, *Hanseniaspora lachancei*, and *Spegazzinia tessarthra* were excessively colonized in the tumor samples, whereas *Preussia persica*, *Fusarium solani*, *Nigrospora oryzae*, *Acremonium furcatum*, *Golovinomyces artemisiae*, and *Tausonia pullulans* were significantly more abundant in tumor-adjacent samples. The fungal co-occurrence network in tumor-adjacent samples was larger and denser than that in tumors. Similarly, the more complex bacterial–fungal interactions in tumor-adjacent samples were also detected. The expression of mechanistic target of rapamycin kinase was positively correlated with the abundance of *N. oryzae* and *T. pullulans* in tumor-adjacent samples. In tumors, the expression of MET proto-oncogene, receptor tyrosine kinase (MET) had a negative correlation and a positive correlation with the abundance of *R. toruloides* and *S. tessarthra*, respectively.

Conclusion   This study revealed the landscape of the esophageal mycobiome characterized by an altered fungal composition and bacterial and fungal ecology in ESCC.

Introduction

Esophageal cancer is the 6th leading cause of death from cancer and the 10th most common cancer in the world [1], with aggressive nature and poor prognosis. Its two main histological types (squamous cell carcinoma and adenocarcinoma) have different incidences and distributions worldwide. Esophageal squamous cell carcinoma (ESCC) shows the highest incidence in China [1] and poses a greater threat to less-developed than developed regions [2]. Tobacco consumption [3], alcohol use [4], and low intake of fruits and vegetables [5] are the major risk factors for ESCC. Further studies are needed to clarify the pathogenesis of ESCC and to explore new diagnostic and therapeutic possibilities.

More attention has been given to the relationship between the microbiome and ESCC in recent years. Yang *et al.* [6] demonstrated that esophageal mucosal microbiota is different between ESCC cases and normal controls. Li *et al.* [7] showed that certain esophageal microbiota dysbiosis has the potential to predict the progression of ESCC. A previous study found that the high abundance of esophageal Streptococcus and Prevotella was associated with poor prognosis in ESCC [8].

In addition to bacterial dysbiosis, alterations in the mycobiota should be considered. The mycobiota, only a small part of the microbiome, has been shown to contribute to disease in a complex manner. Wheeler and his colleagues [9] suggested that the fungal community in the gut is important for modulating immune function in colon diseases. Intestinal fungal dysbiosis has been observed in patients with alcoholic hepatitis [10]. Papon *et al.* [11] indicated that the gastric fungal imbalance was associated with gastric cancer. These observations suggest that mycobiota dysbiosis could be an important factor in the development or progression of gastrointestinal diseases. However, unlike bacteria, little is known about the role of fungi within the esophageal microbiota. In this study, we used non-culture-based high-throughput amplicon sequencing to characterize the esophageal mycobiota in tumor and tumor-adjacent samples from patients with ESCC. The co-occurrence network between two tissues and cross-domain association of bacterial and fungal communities was also investigated. Finally, we elucidated the associations between the expression of pathogenic genes including MET proto-oncogene, receptor tyrosine kinase (MET) and mechanistic target of rapamycin kinase (MTOR), and differential mycobiota.

Materials and methods

Study population

We performed a hospital-based retrospective study in patients pathologically diagnosed with primary ESCC between February 2015 and October 2020 at Fujian Provincial Cancer Hospital (Fuzhou, Fujian, China) and Zhangzhou Municipal Hospital (Zhangzhou, Fujian, China). Subjects were chosen according to the following criteria. Inclusion criteria: (i) underwent esophagectomy; (ii) pathologically diagnosed with primary ESCC; (iii) tumor stage clarified with number of harvested lymph nodes of ≥20; (iv) undergoing neither preoperative radiotherapy nor chemotherapy; (v) no record of other infectious diseases; and (vi) resident of Fujian province for >10 years. Exclusion criteria: (i) incomplete clinicopathological data and non-availability of

tissue samples; (ii) metastatic malignancy or recurrent esophageal cancer; (iii) had received pharmacotherapy (such as oral, intramuscular, and intravenous antibacterial drugs, various probiotics, or other drugs affecting the microbiota) within 2 months. All procedures performed in studies involving human participants were carried out by the ethical standards of the institutional and/or national research committee, and with the 1964 Helsinki Declaration and its later amendments or comparable ethical standards. Written informed consent was obtained from all the patients. The study was approved by the Ethics Committee of Fujian Medical University (approval No. 201495).

Demographic and clinical information

The basic information of all the participants was collected from their medical records and through a detailed questionnaire evaluating sociodemographic status and clinicopathological features (i.e. tumor location and tumor, node, and metastasis [TNM] stage).

Sample collection and preservation

Paired tumor and tumor-adjacent samples were obtained from patients with ESCC immediately after surgical resection in the operating room. The tumor-adjacent samples were obtained from an area at a distance of 3 cm from the cancerous tissue. The samples were cut into small pieces and placed in autoclaved cryovials, stored in liquid nitrogen for 1 h, and then transferred to a −80°C freezer for storage. All samples were evaluated by using pathological hematoxylin and eosin staining.

Microbial DNA extraction and sequencing

All samples were lysed by using vortex with lysozyme and glass beads (mixed with 1.0 mm and 0.5 mm). The microbial DNA was extracted using a Mag Maxi Kit (LGC; Berlin, Germany). The extracted DNA of paired tumor and tumor-adjacent tissues from patients was quantitatively detected by using a Qubit fluorometer (Invitrogen; Carlsbad, CA, USA); only those with Internal Transcribed Spacer Region (ITS) region amplification and available libraries were acceptable. Each extraction was performed using a blank buffer control to detect contaminants from either reagent or other unintentional sources. Too little DNA was detected in the negative controls to prepare libraries; hence, these samples were not sequenced.

The V3–V4 region of 16S ribosomal Ribonucleic Acid (RNA) (rRNA; representing bacteria) and the internal transcribed spacer region 1 (ITS1) rRNA (representing fungi) were amplified with the following primers (for 16S rRNA, primers 341F: 5′-CCTAYGGGRBGCASCAG-3′ and 806R: 5′-GGACTACNNGGGTATCTAAT-3′; for ITS1 rRNA, primers 1F-F: 5′-CTTGGTCATTTAGAGGAAGTAA-3′ and 1F-R: 5′-GCTGCGTTCTTCATCGATGC-3′). The sequencing platform was the HiSeq2500 PE250 (Illumina; San Diego, CA, USA).

Quantitative reverse transcription PCR

Total RNA was extracted using TRIzol total RNA isolation reagent (Hunan Accurate Bio-Medical Co., Ltd; Changsha, Hunan, China). RNA was used to reverse transcribe complementary

DNA (cDNA) using an Evo M-MLV RT Kit with gDNA Clean for qPCR (Hunan Accurate Bio-Medical Co., Ltd). *Fusarium solani* (forward primer, 5′-ATCTCTTGGCTCTGGCATC-3′; reverse primer, 5′-ACATTACTTATCGCATTTCGC-3′), *MET* (forward primer, 5′-TCAGGAGGTGTTTGGAAAG-3′; reverse primer, 5′-GCAGTATG ATTGTGGGGAA-3′), *MTOR* (forward primer, 5′-GTTGGCCCTCA CCTCAC-3′; reverse primer, 5′-CTTGGCAGCTCTCTCACC-3′), and *GAPDH* (forward primer, 5′-GCACCGTCAAGGCTGAGAAC-3′; reverse primer, 5′-TGGTGAAGACGCCAGTGGA-3′) mRNA levels were measured by using quantitative reverse transcription PCR (qRT-PCR). Amplification was performed using the ABI QuantStudio™ 5 RealTime Polymerase Chain Reaction (PCR) system (Applied Biosystems; Foster City, CA, USA) using the following reaction conditions: 95°C for 30 s followed by 40 cycles of 95°C for 5 s and 60°C for 30 s.

Sequence data processing

The bacterial analysis of samples from patients with ESCC was performed using the modified methods described in our previous reports [12]. Raw ITS sequencing data were imported into Quantitative Insights Into Microbial Ecology (QIIME2-2020.02) [13] and processed using the DADA2 algorithm to denoise and then inferred exact amplicon sequence variants (ASVs). The retained ASVs were aligned and annotated by using the Naïve Bayes classifier using the UNITE (version 2020.4) database. Before diversity analysis, the threshold for rarefaction depth was determined by minimizing sequence loss while maximizing the number of samples. At a depth of 10,000 sequences per sample, the richness of the observed communities had tended to be saturated, with 84 tumor and tumor-adjacent samples kept for the alpha and beta diversity metric construction. To provide better resolution and limit the false discovery rate penalty on statistical tests, the low abundance features (with total ASV counts of <50 or detected in fewer than five samples) were filtered before the differential abundance analysis.

Statistical analysis

Questionnaires and clinicopathological data were entered twice into EpiData (version 3.1; Odense, Syddanmark, Denmark). The demographic and baseline clinical features are presented as numbers of cases followed by percentages in parentheses. All statistical analyses were performed using R software (R version 4.0.4) and results with a two-tailed $P < 0.05$ were considered statistically significant.

The Wilcoxon rank-sum test was applied for comparisons of alpha diversity (observed ASVs, Shannon index, and evenness) between tumor and tumor-adjacent samples. The beta diversity was examined by using the one-way permutational multivariate analysis of variance comparison of Bray–Curtis and Jaccard distance matrices. Additionally, the Adonis tests were performed to evaluate whether the variation in distances could be explained by other controlled variables (sampling season, residential region, tumor location, and TNM stage). Principal coordinates analysis (PCoA) plotting, which was based on the Bray–Curtis and Jaccard distances, were used to depict the microbiome composition. The analysis of composition of microbiomes II (ANCOM-II) [14] was performed to detect the differential abundance in different sample groups.

The strength of the edges of the fungal co-occurrence network was assessed by using the SparCC [15] algorithm and the interaction network diagram was visualized using Cytoscape [16]. The top hub taxa were assessed by using the cytoHubba

plugin [17] in Cytoscape. The cross-domain association of bacterial and fungal communities was calculated and visualized by using the NetCoMi R package [18].

Results

Study participant characteristics

A total of 92 esophageal tissues were obtained from 66 patients with ESCC in this study. These patients' baseline demographic and clinical information is presented in Supplementary Table 1. The most patients with ESCC in this study were male ($n = 50$). Approximately 40.9% of patients had Stage I/II ESCC.

Mycobiota communities in cancer tissue differ from those in adjacent tissue

Unlike in the tumor samples, tumor-adjacent samples showed a significantly higher mycobiota alpha diversity (observed ASVs, $P = 0.001$; Shannon index, $P = 0.013$; Figure 1A–C). The PCoA displayed that the tumor tissues could be grouped separately from tumor-adjacent samples, which indicated that changes in the fungal communities might be one of the factors influencing the disease (Bray–Curtis distance, $P_{anova} = 0.001$, Figure 1D; Jaccard distance, $P_{anova} = 0.001$, Figure 1E). Multivariate Adonis analysis suggested that sample type accounted for 1%–3% of the variation within mycobiota beta diversity to some extent (Figure 1F and G). A detailed comparison of the relative abundance of fungi in the tumor and tumor-adjacent samples (Supplementary Figure 1A) showed that the phyla Ascomycota and Basidiomycota dominated in both groups and the proportions of Basidiomycota were higher in tumors than in tumor-adjacent samples. Among the most dominant genera, Cladosporium, Aspergillus, and Pseudallescheria were more abundant in tumors than in tumor-adjacent samples (Supplementary Figure 1B).

Altered mycobiota in different tissues

The fungi comparison between tumor and tumor-adjacent samples using the ANCOM-II algorithm (Table 1) revealed that abundance of Ascomycota was higher than that of Basidiomycota in both groups. Among the top three high-abundant species (*Hanseniaspora lachancei*, *Spegazzinia tessarthra*, and *F. solani*) in Ascomycota, *F. solani* were significantly more abundant in tumor-adjacent samples than in tumors. The phylum Basidiomycota was dominant in tumors, which may primarily have been due to the abundance of *Rhodotorula toruloides* and *Malassezia dermatis*.

Fungal co-occurrence network analysis

To investigate the interaction among esophageal fungi in tumor and tumor-adjacent samples, we constructed the fungal co-occurrence networks of two groups (Figure 2). The network of tumor-adjacent samples was obviously larger and denser than that of tumors. The top five hub taxa in tumor samples were from the phyla Ascomycota, Mortierellomycota, and Rozellomycota, whereas those in tumor-adjacent samples were from phyla Ascomycota and Basidiomycota. Interestingly, the differential species *Preussia persica* played an important role in both networks.

Cross-domain association of bacterial and fungal communities

To explore interactions among members of the esophageal bacterial and fungal species in patients with ESCC, we used
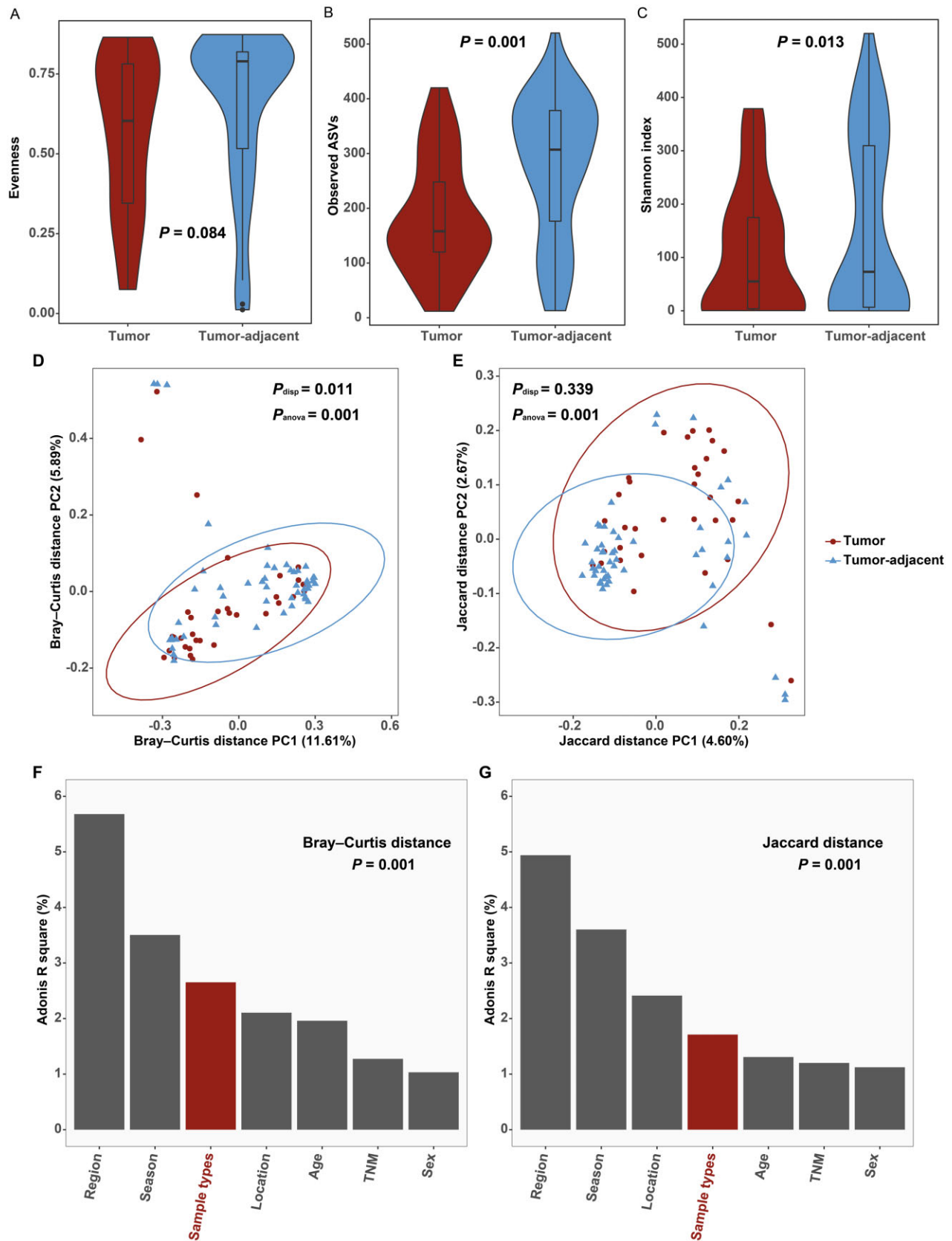
Figure 1. The mycobiota diversity in tumor and tumor-adjacent samples in ESCC. (A)–(C) Mycobiota alpha diversity including (A) the evenness index, (B) observed ASVs index, and (C) Shannon index. (D) and (E) Univariate and multivariate analyses of mycobiota beta diversity including (D) PCoA plots based on Bray–Curtis distance and (E) PCoA plots based on Jaccard distance. (F) and (G) Bar plot of Adonis R square based on Bray–Curtis distance (F) and Jaccard distance (G) adjusted by residential region, sampling season, sample type, tumor location, age, TNM stage, and sex.

Table 1. Differential fungi between tumor and tumor-adjacent samples in ESCC selected by using ANCOM-II[a]

Phylum	Class	Order	Family	Genus	Species	W value	Relative abundance		Fold change[b]
							Tumor	Tumor-adjacent	
Ascomycota	Sordariomycetes	Sordariales	–	–	–	186	8.05E-04	3.00E-03	0.268
Ascomycota	Sordariomycetes	Hypocreales	Nectriaceae	–	–	203	1.80E-02	3.50E-02	0.514
Ascomycota	Dothideomycetes	Pleosporales	Sporormiaceae	*Preussia*	*P. persica*	187	3.00E-03	7.00E-03	0.429
Ascomycota	Saccharomycetes	Saccharomycetales	Saccharomycodaceae	*Hanseniaspora*	*H. lachancei*	256	1.93E-01	1.23E-04	1,569.106
Ascomycota	Sordariomycetes	Hypocreales	Nectriaceae	*Fusarium*	*F. solani*	205	8.00E-03	1.70E-02	0.471
Ascomycota	Sordariomycetes	Trichosphaeriales	Trichosphaeriaceae	*Nigrospora*	*N. oryzae*	Inf	0	2.26E-04	0
Ascomycota	Sordariomycetes	Hypocreales	Hypocreales_fam_Incertae_sedis	*Acremonium*	*A. furcatum*	Inf	0	8.28E-04	0
Ascomycota	Leotiomycetes	Erysiphales	Erysiphaceae	*Golovinomyces*	*G. artemisiae*	Inf	9.03E-07	7.91E-05	0.011
Ascomycota	Dothideomycetes	Pleosporales	Didymosphaeriaceae	*Spegazzinia*	*S. tessarthra*	225	3.06E-03	4.85E-04	6.313
Basidiomycota	Microbotryomycetes	Sporidiobolales	Sporidiobolaceae	*Rhodotorula*	*R. toruloides*	209	4.00E-03	4.03E-04	9.926
Basidiomycota	Tremellomycetes	Cystofilobasidiales	Mrakiaceae	*Tausonia*	*T. pullulans*	184	2.06E-04	2.00E-03	0.103
Basidiomycota	Malasseziomycetes	Malasseziales	Malasseziaceae	*Malassezia*	*M. dermatis*	232	6.98E-04	3.12E-05	22.372

[a]Adjusted by sex, age, TNM stage, sampling season, tumor location, and residential region.
[b]Fold change = tumor relative abundance/tumor-adjacent relative abundance.
ESCC, esophageal squamous cell carcinoma; ANCOM-II, analysis of composition of microbiomes II; Inf, infinity.
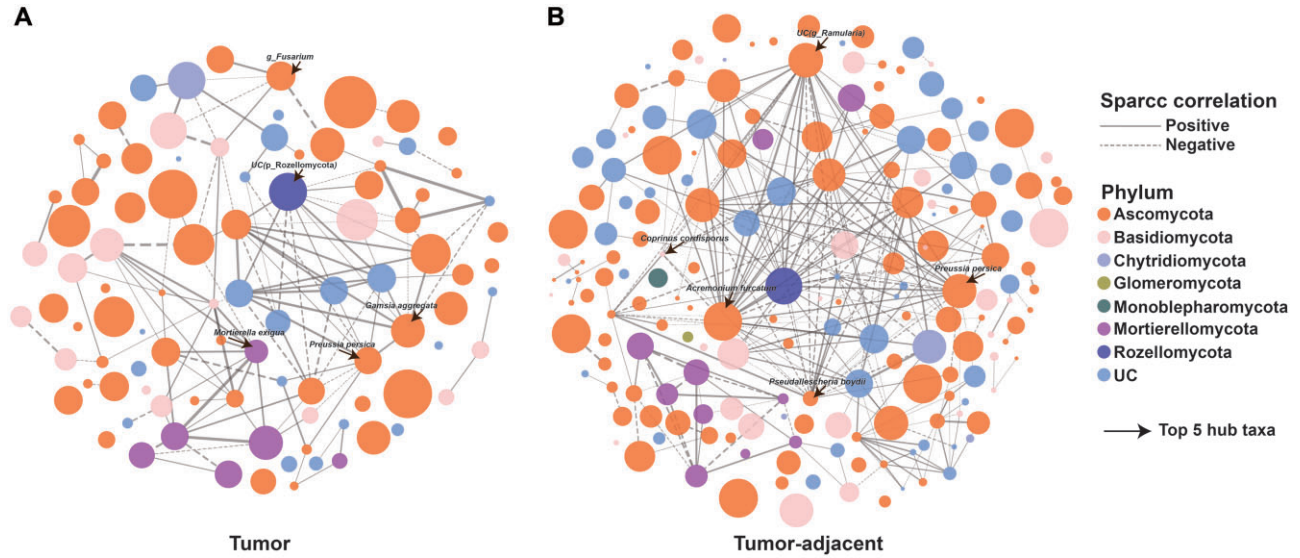
Figure 2. Fungal co-occurrence network in ESCC. Separate network plots were generated for (A) tumor and (B) tumor-adjacent samples. Nodes represent amplicon sequence variants (ASVs) involved in fungi. The size of each node denotes the centered log-ratio transformation of the abundance of each ASV. The edges indicate the SparCC correlations (solid line, positive; dotted line, negative); the line thickness corresponds to the strength of the association. Only significant correlations (two-sided pseudo $P \leq 0.05$ based on bootstrapping of 1,000 repetitions) with an absolute correlation magnitude of ≥ 0.4 or ≤ -0.4 are presented for visual clarity. "UC" means the unclassified mycobiota according to the database.
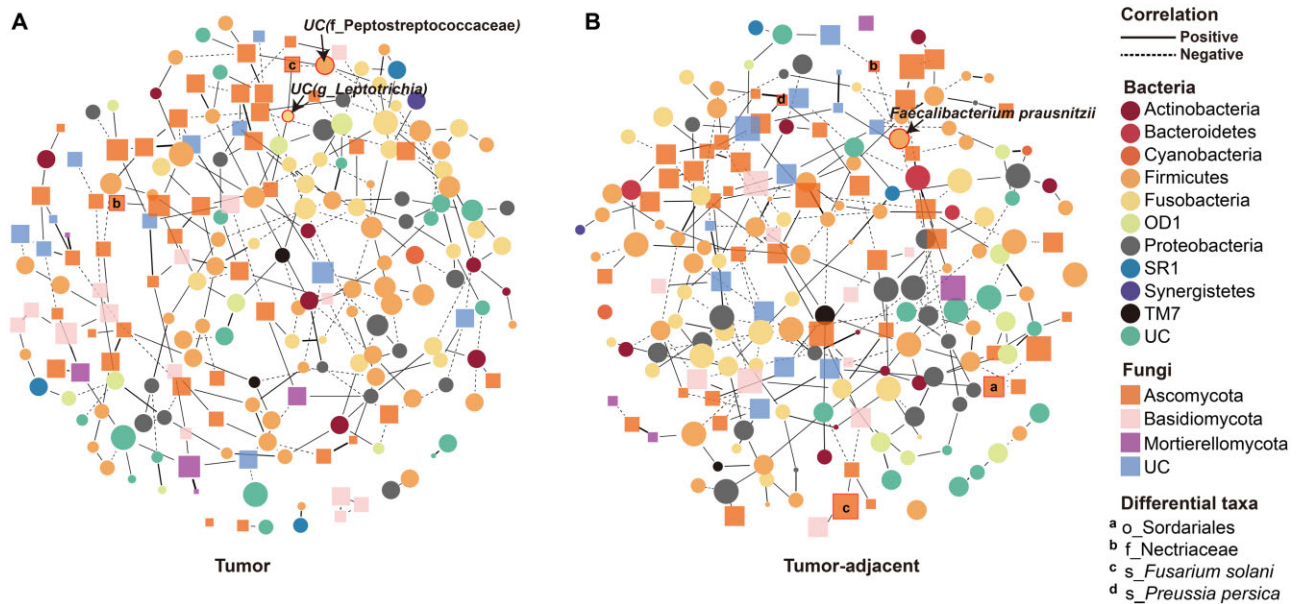

Figure 3. The potential cross-domain interactions between tumor (A) and tumor-adjacent (B) samples in ESCC. Nodes represent features involved in bacteria (circle) or fungi (square). The color of each node indicates the phylum of the feature; the size denotes the degree centrality of each feature. The edges indicate the correlations (solid line, positive; dotted line, negative); the line thickness corresponds to the strength of the association. Only correlations with an absolute correlation magnitude ≥ 0.25 or ≤ -0.25 are presented for visual clarity. "UC" means the unclassified microbiota according to the database.

NetCoMi to build correlation networks of abundant taxa and analysed both bacterial and fungal communities in 39 samples performing both 16S sequencing and ITS sequencing (Figure 3). The fungal and bacterial co-occurrence network in tumor-adjacent samples was denser than that in tumors. The above differential mycobiota also participated in both networks.

Notably, *F. solani* abundance exhibited a positive correlation with the abundance of unclassified species in the genus *Leptotrichia* and negative with the abundance of unclassified species in the family Peptostreptococcaceae in tumor samples. However, no correlation was observed between the abundance of *F. solani* and any bacteria in tumor-adjacent samples. The
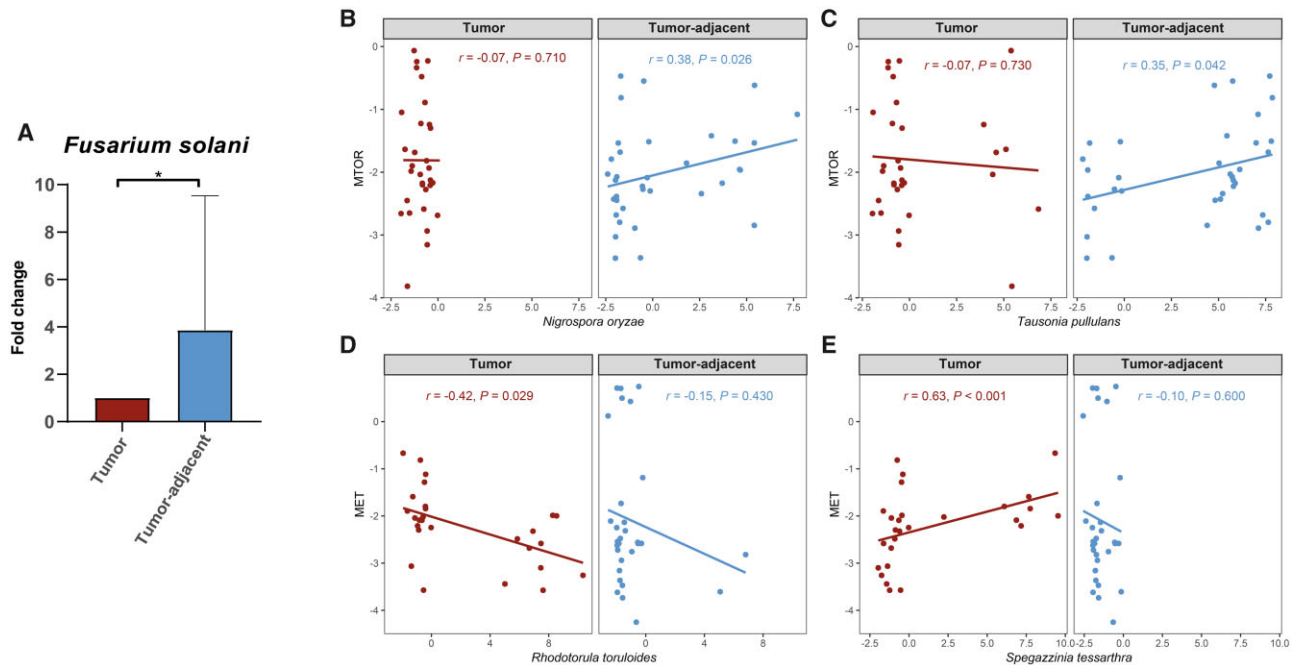
Figure 4. The association between the expression of MET and MTOR and differential mycobiota. (A) The abundance of *Fusarium solani* in tumor vs that in paired tumor-adjacent samples. (B)–(E) The abundance of differential mycobiota associated with the mRNA expression of MTOR and MET. (B) MTOR mRNA and *Nigrospora oryzae*; (C) MTOR mRNA and *Tausonia pullulans*; (D) MET mRNA and *Rhodotorula toruloides*; (E) MET mRNA and *Spegazzinia tessarthra*.

abundance of the family Nectriaceae showed a negative correlation with that of *Faecalibacterium prausnitzii* in tumor-adjacent samples. In tumors, only the within-domain correlations were found between the Nectriaceae family and other members of fungi. Taken together, these results suggested complex and close bacterial–fungal interactions in the esophageal microbiota in patients with ESCC. Consequently, we could infer that the taxa might have different clusters in different tissues.

The association between the expression of MET and MTOR and differential fungi

To validate the species we identified as differentially abundant in ESCC from our ITS1-based microbiome analyses, we quantified the presence of *F. solani*. An increase in *F. solani* abundance in tumor-adjacent samples (Figure 4A) is consistent with the result of the altered abundance of this species by ITS1-based analyses. Next, we evaluated the association between the levels of reported pathogenic genes and differential fungi using Spearman correlation analysis (Figure 4B–E). The results suggested that the abundance of *Nigrospora oryzae* ($r = 0.38$, $P = 0.026$, Figure 4B) and *Tausonia pullulans* ($r = 0.35$, $P = 0.042$, Figure 4C) in tumor-adjacent samples were positively correlated with the expression of MTOR. The abundance of *R. toruloides* ($r = -0.42$, $P = 0.029$, Figure 4D) in tumors exhibited a negative correlation with the expression of MET. The abundance of *S. tessarthra* ($r = 0.63$, $P < 0.001$, Figure 4E) in tumors had a positive correlation with the expression of MET.

Discussion

In this study, we investigated the landscape of fungi associated with ESCC. Investigating the colonization of tissue samples can better demonstrate the microbial characteristics in the surrounding environment in the context of esophageal carcinogenesis than analysing fecal samples [19]. Therefore, we utilized high-throughput ITS1 and 16S sequencing of fungal and bacterial ribosomal DNA to explore distinct mycobiota patterns and altered bacterial–fungal interactions in the esophagus of patients with ESCC, which is a relatively young research field in the context of the esophageal microbiome dysbiosis in ESCC.

The tumor samples showed a lower species richness and diversity than did the tumor-adjacent samples. This finding is in agreement with that reported by Zhong *et al.*, who found that the fungal alpha diversity in gastric cancer lesions was significantly lower than that in adjacent non-cancerous tissues [20]. Similarly, significantly lower diversity of intestinal fungi in patients than in healthy controls was also demonstrated [21].

Additionally, the mycobiota beta diversity between subjects suggested that except for the effect of different tissues, the host residential regions accounted for the most variation. This finding was consistent with the influence of geographic variations [22]; geography has been considered a potential factor structuring the gut mycobiota. Besides, seasonal variation related to meteorological conditions might account for changes in the mycobiota composition [23]. In addition, our stratified analyses (Supplementary Figures 2–4) suggested the difference in diversity and fungi between tumor and tumor-adjacent samples are also observed in different regions and seasons.

Notably, we identified specific fungal composition changes in ESCC. At the phylum level, Ascomycota and Basidiomycota were the most enriched in the tumor samples compared with the tumor-adjacent samples, while Chytridiomycota was less enriched. Indeed, these two dominant taxa, Ascomycota and Basidiomycota, accounted for >80% of the fungi in all samples. This observation is consistent with the mycobiota composition in the environment and may reflect the fact that esophageal mycobiota constituents are derived from ingestion [24]. We

further analysed the differences between the two sample types and, at the species level, which confirmed that *R. toruloides*, *M. dermatis*, *H. lachancei*, and *S. tessarthra* were excessively colonized in the tumor samples, whereas *P. persica*, *F. solani*, *N. oryzae*, *Acremonium furcatum*, *Golovinomyces artemisiae*, and *T. pullulans* were significantly more abundant in tumor-adjacent samples. *Rhodotorula toruloides* is a robust producer of fatty acids biosynthesis owing to its fast growth and strong metabolic flux under conditions of high abundance [25]. Moreover, previous studies reported that *R. toruloides* [26] and the species in *Preussia* [27] might be involved in glucose metabolism and the specific mechanism remains to be confirmed [28]. These microorganisms might be implicated in the metabolic perturbations involved in promoting tumor formation in ESCC. Han *et al.* [29] reported that *M. dermatis* was more abundant in adult patients with atopic dermatitis than that in healthy controls, while levels of other *Malassezia* species were not significantly altered. It is possible that this fungus participated in host inflammation. Peters and his colleagues [30] determined that a higher abundance of *Fusarium* species was found in samples from participants with good oral health than in participants with periodontal disease, which is similar to our results in ESCC that this microbe was more abundant in tumor-adjacent samples than in tumor samples. Future research is needed to clarify whether these differential fungi are commensals in the esophagus or whether they are introduced via the environment, as well as to determine their role in ESCC.

Here, the tumor-adjacent ecological network showed more abundant fungi and denser correlations than that in tumors in ESCC, which was consistent with a previous bacterial study on gastric cancer [31]. This finding reveals that the process of carcinogenesis may alter the esophageal microenvironment, reduce the interaction of microorganisms, and hasten cancer progression. Interestingly, several hub fungi showed the most association with others in the networks. Among these, the complex interactions formed by *P. persica* showed the high centralities in the two networks. In addition, the mycobiota differed between tumor and tumor-adjacent tissue. These findings indicate that even the same fungi in different tissues displayed important roles.

Fungi and bacteria cohabit and interact with each other in the human and animal gastrointestinal tract [32, 33]. Increased or decreased levels of fungi were observed in mice after antibiotic treatment or after cessation of antibiotic treatment, suggesting a balance between fungal and bacterial microbiota [34]. Cross-domain correlations in community composition dissimilarities between tumor and tumor-adjacent samples in ESCC were detected in this study. Our findings showed that a high abundance of *F. solani* and Firmicutes coexisted in the esophagus, which is in agreement with observations of the intestine [35]. From a clinical perspective, cross-domain relationships have been proven to affect the physiology, pathogenicity, and virulence of organisms, and their interaction with the host's immunity [36, 37]. These significant correlations observed may be biologically important for the microbiota and hosts. Therefore, future longitudinal analyses of the esophageal mycobiome will extend our understanding of the role of bacterial and fungal organisms in the etiology and pathogenesis of ESCC.

Expression of several markers, e.g. MET [38] and MTOR [39], may play a role in the development of ESCC. However, the mechanism of esophageal dysbiosis of the mycobiota involved in ESCC carcinogenesis is still uncertain. In the current study, the levels of MTOR and MET were associated with the abundance of *N. oryzae*, *T. pullulans*, *R. toruloides*, and *S. tessarthra*.

Interestingly, the relative abundances of *N. oryzae* and *T. pullulans* were richer in tumor-adjacent samples and also positively correlated with MTOR expression. It could be speculated that high levels of fungi and MTOR in non-cancer tissues may interact to promote ESCC development. Furthermore, the higher abundance of *S. tessarthra* in cancer is strongly positively associated with MET expression, suggesting that the mycobiota in the tumor microenvironment can affect gene expression and further influence ESCC.

This study investigated the esophageal mycobiota landscape and the combined exploration of esophageal bacterial and fungal communities in patients with ESCC. However, this study still had several limitations. Major limiting factors were the small sample size and heterogeneous sampling across regions and seasons. Another limiting factor was the observational study design, which provides only the possible statistical relationships among cross-domain microbes. Therefore, future *in vivo* and *in vitro* experiments are required to confirm the potential mechanism linking these microorganisms with the host.

In conclusion, this study comprehensively described the characteristics of the esophageal mycobiota, the ecology of fungi, and the interkingdom interaction of bacteria and fungi. Moreover, the abundance of several dysbiotic fungi was correlated with the expression of the carcinogenic genes MTOR and MET, which revealed the possible mechanisms involved in the development of ESCC.

Supplementary Data

Supplementary data is available at *Gastroenterology Report* online.

Authors' Contributions

W.Q.R., Z.L., and Z.J.H. conceived and designed the project. W.Q.R., J.J., J.W.W., and Y.M.C. collected the data. W.Q.R., Z.L., J.J., Z.F.L., R.F., W.L.C., X.E.P., and Z.J.H. analysed and interpreted the data. W.Q.R. and Z.L. drafted the manuscript. All authors read and approved the final manuscript.

Funding

Acknowledgements

Conflict of Interest

None declared.

Data availability

The data sets during the current study are available from the corresponding author on reasonable request.

References

[1]. Sung H, Ferlay J, Siegel RL et al. Global Cancer Statistics 2020: GLOBOCAN estimates of incidence and mortality worldwide for 36 cancers in 185 countries. *CA Cancer J Clin* 2021;**71**: 209–49.

[2]. Ferlay J, Soerjomataram I, Dikshit R et al. Cancer incidence and mortality worldwide: sources, methods and major patterns in GLOBOCAN 2012. *Int J Cancer* 2015;**136**:E359–86.

[3]. Wang G, Ye M, Zheng S et al. Cigarette smoke extract induces H19 in esophageal squamous cell carcinoma in smoking patients: based on a chronic exposed cell model. *Toxicol Lett* 2020;**333**:62–70.

[4]. Li XC, Wang MY, Yang M et al. A mutational signature associated with alcohol consumption and prognostically significantly mutated driver genes in esophageal squamous cell carcinoma. *Ann Oncol* 2018;**29**:938–44.

[5]. Sheikh M, Poustchi H, Pourshams A et al. Individual and combined effects of environmental risk factors for esophageal cancer based on results from the Golestan cohort study. *Gastroenterology* 2019;**156**:1416–27.

[6]. Yang W, Chen CH, Jia M et al. Tumor-associated microbiota in esophageal squamous cell carcinoma. *Front Cell Dev Biol* 2021;**9**:641270.

[7]. Li M, Shao D, Zhou J et al. Signatures within esophageal microbiota with progression of esophageal squamous cell carcinoma. *Chin J Cancer Res* 2020;**32**:755–67.

[8]. Liu Y, Lin Z, Lin Y et al. Streptococcus and Prevotella are associated with the prognosis of oesophageal squamous cell carcinoma. *J Med Microbiol* 2018;**67**:1058–68.

[9]. Wheeler ML, Limon JJ, Bar AS et al. Immunological consequences of intestinal fungal dysbiosis. *Cell Host Microbe* 2016; **19**:865–73.

[10]. Lang S, Duan Y, Liu J et al. Intestinal fungal dysbiosis and systemic immune response to fungi in patients with alcoholic hepatitis. *Hepatology* 2020;**71**:522–38.

[11]. Papon N, Hohl TM, Zhai B. Mycobiota dysbiosis and gastric tumorigenesis. *Theranostics* 2021;**11**:7488–90.

[12]. Lin Z, Rao W, Xiang Z et al. Characteristics and interplay of esophageal microbiota in esophageal squamous cell carcinoma. *BMC Cancer* 2022;**22**:696.

[13]. Bolyen E, Rideout JR, Dillon MR et al. Reproducible, interactive, scalable and extensible microbiome data science using QIIME 2. *Nat Biotechnol* 2019;**37**:852–7.

[14]. Kaul A, Mandal S, Davidov O et al. Analysis of microbiome data in the presence of excess zeros. *Front Microbiol* 2017;**8**:2114.

[15]. Friedman J, Alm EJ. Inferring correlation networks from genomic survey data. *PLoS Comput Biol* 2012;**8**:e1002687.

[16]. Smoot ME, Ono K, Ruscheinski J et al. Cytoscape 2.8: new features for data integration and network visualization. *Bioinformatics* 2011;**27**:431–2.

[17]. Chin CH, Chen SH, Wu HH et al. cytoHubba: identifying hub objects and sub-networks from complex interactome. *BMC Syst Biol* 2014;**8** Suppl 4:S11.

[18]. Peschel S, Müller CL, von Mutius E et al. NetCoMi: network construction and comparison for microbiome data in R. *Brief Bioinform* 2021;**22**:bbaa290.

[19]. Rezasoltani S, Dabiri H, Asadzadeh-Aghdaei H et al. The gut microflora assay in patients with colorectal cancer: in feces or tissue samples? *Iran J Microbiol* 2019;**11**:1–6.

[20]. Zhong M, Xiong Y, Zhao J et al. Candida albicans disorder is associated with gastric carcinogenesis. *Theranostics* 2021;**11**: 4945–56.

[21]. Li M, Dai B, Tang Y et al. Altered bacterial-fungal interkingdom networks in the guts of ankylosing spondylitis patients. *mSystems* 2019;**4**:e00176-18.

[22]. Kabwe MH, Vikram S, Mulaudzi K et al. The gut mycobiota of rural and urban individuals is shaped by geography. *BMC Microbiol* 2020;**20**:257.

[23]. Vitte J, Michel M, Malinovschi A et al.; EAACI Task Force on Allergic Bronchopulmonary Aspergillosis. Fungal exposome, human health, and unmet needs: a 2022 update with special focus on allergy. *Allergy* 2022;**77**:3199–216.

[24]. Richard ML, Sokol H. The gut mycobiota: insights into analysis, environmental interactions and role in gastrointestinal diseases. *Nat Rev Gastroenterol Hepatol* 2019;**16**: 331–45.

[25]. Liu Y, Koh CMJ, Yap SA et al. Understanding and exploiting the fatty acid desaturation system in Rhodotorula toruloides. *Biotechnol Biofuels* 2021;**14**:73.

[26]. Hsiao HY, Chiang LC, Ueng PP et al. Sequential utilization of mixed monosaccharides by yeasts. *Appl Environ Microbiol* 1982;**43**:840–5.

[27]. Rangel-Grimaldo M, Rivero-Cruz I, Madariaga-Mazón A et al. α-Glucosidase inhibitors from Preussia minimoides ‡. *J Nat Prod* 2017;**80**:582–7.

[28]. Xu J, Zhang Y, Wang X et al. Changes and roles of intestinal fungal microbiota in coronary heart disease complicated with nonalcoholic fatty liver disease. *Am J Transl Res* 2020; **12**:3445–60.

[29]. Han SH, Cheon H I, Hur MS et al. Analysis of the skin mycobiome in adult patients with atopic dermatitis. *Exp Dermatol* 2018;**27**:366–73.

[30]. Peters BA, Wu J, Hayes RB et al. The oral fungal mycobiome: characteristics and relation to periodontitis in a pilot study. *BMC Microbiol* 2017;**17**:157.

[31]. Chen XH, Wang A, Chu AN et al. Mucosa-associated microbiota in gastric cancer tissues compared with non-cancer tissues. *Front Microbiol* 2019;**10**:1261.

[32]. Lee SC. mSphere of influence: the mycobiota in human health and disease. *mSphere* 2020;**5**:e00974-19.

[33]. Doron I, Leonardi I, Iliev ID. Profound mycobiome differences between segregated mouse colonies do not influence Th17 responses to a newly introduced gut fungal commensal. *Fungal Genet Biol* 2019;**127**:45–9.

[34]. Dollive S, Chen YY, Grunberg S et al. Fungi of the murine gut: episodic variation and proliferation during antibiotic treatment. *PLoS One* 2013;**8**:e71806.

[35]. Scupham AJ, Presley LL, Wei B et al. Abundant and diverse fungal microbiota in the murine intestine. *Appl Environ Microbiol* 2006;**72**:793–801.

[36]. Peters BM, Jabra-Rizk MA, O'May GA et al. Polymicrobial interactions: impact on pathogenesis and human disease. *Clin Microbiol Rev* 2012;**25**:193–213.

[37]. Leung MHY, Chan KCK, Lee PKH. Skin fungal community and its correlation with bacterial community of urban Chinese individuals. *Microbiome* 2016;**4**:46.

[38]. Lin DC, Wang MR, Koeffler HP. Genomic and epigenomic aberrations in esophageal squamous cell carcinoma and implications for patients. *Gastroenterology* 2018;**154**:374–89.

[39]. Dong D, Zhang W, Xiao W et al. A GRN autocrine-dependent FAM135B/AKT/mTOR feedforward loop promotes esophageal squamous cell carcinoma progression. *Cancer Res* 2021; **81**:910–22.